OPEN BIOLOGY

royalsocietypublishing.org/journal/rsob



Research

**Cite this article:** Xu J *et al*. 2025 Unravelling axonal transcriptional landscapes: insights from induced pluripotent stem cell-derived cortical neurons and implications for motor neuron degeneration. *Open Biol.* **15**: 250101.
https://doi.org/10.1098/rsob.250101

Received: 3 April 2025
Accepted: 9 May 2025

**Subject Areas:**
neuroscience, structural biology, molecular biology, cellular biology, biochemistry

**Keywords:**
axonal transcriptomics, transcription factors, axonal transport, kinesin, neurons, iPSC-derived neurons

**Author for correspondence:**
Rebecca Schuele
e-mail: rebecca.schuele@uni-heidelberg.de



# Unravelling axonal transcriptional landscapes: insights from induced pluripotent stem cell-derived cortical neurons and implications for motor neuron degeneration

Jishu Xu[1,2,3,4,†,‡], Michaela Hörner[4,†,‡], Maike Nagel[1], Perwin Perhat[4], Milena Korneck[1,3,5,6], Marvin Noß[1], Stefan Hauser[1,5,6], Ludger Schoels[1,5,6], Jakob Admard[2], Nicolas Casadei[2] and Rebecca Schuele[1,4]

[1]Eberhard Karls University Tübingen Hertie Institute for Clinical Brain Research, Tübingen, Baden-Württemberg, Germany
[2]Institute of Medical Genetics and Applied Genomics, and [3]Graduate School of Cellular and Molecular Neuroscience, University of Tübingen, Tübingen, Baden-Württemberg, Germany
[4]Division of Neurodegenerative Diseases and Movement Disorders, Department of Neurology, Heidelberg University Hospital, Heidelberg, Baden-Württemberg, Germany
[5]German Centre for Neurodegenerative Diseases, Tübingen, Baden-Württemberg, Germany
[6]Department of Neurology, University Hospital Tübingen, Tübingen, Baden-Württemberg, Germany

MH, 0000-0001-5485-4990; RS, 0000-0002-7781-2766

Neuronal function and pathology are deeply influenced by the distinct molecular profiles of the axon and soma. Traditional studies have often overlooked these differences due to the technical challenges of compartment-specific analysis. In this study, we employ a robust RNA-sequencing approach, using microfluidic devices, to generate high-quality axonal transcriptomes from induced pluripotent stem cells-derived cortical neurons (CNs). We achieve high specificity of axonal fractions, ensuring sample purity without contamination. Comparative analysis revealed a unique and specific transcriptional landscape in axonal compartments, characterized by diverse transcript types, including protein-coding mRNAs, RNAs encoding ribosomal proteins, mitochondrial-encoded RNAs and long non-coding RNAs. Previous works have reported the existence of transcription factors (TFs) in the axon. Here, we detect a set of TFs specific to the axon and indicative of their active participation in transcriptional regulation. To investigate transcripts and pathways essential for central motor neuron (MN) degeneration and maintenance we analysed kinesin family member 1C (*KIF1C*)-knockout (*KO*) CNs, modelling hereditary spastic paraplegia, a disorder associated with prominent length-dependent degeneration of central MN axons. We found that several key factors crucial for survival and health were absent in *KIF1C-KO* axons, highlighting a possible role of these also in other neurodegenerative diseases. Taken together, this study underscores the utility of microfluidic devices in studying compartment-specific transcriptomics in human neuronal models and reveals complex molecular dynamics of axonal biology. The impact of *KIF1C* on the axonal transcriptome not only deepens our understanding of MN diseases but also presents a promising avenue for exploration of compartment-specific disease mechanisms.

[†]These authors contributed equally to the study.
[‡]Joint first authors.

Electronic supplementary material is available online at http://doi.org/10.6084/m9.figshare.c.7819460.

THE ROYAL SOCIETY PUBLISHING

## 1. Introduction

The inaccessibility of the brain makes analysis of homeostatic and disease conditions challenging. However, understanding these conditions and their pathological mechanisms is a prerequisite for developing targeted therapies for diseases of the central nervous system (CNS). Even though considerable research goes into the development of novel therapeutic approaches for common and rare neurodegenerative diseases, many are still without cure. Up to now, it is mostly post-mortem-derived brain tissue that has been analysed, where preservation of RNA, protein, DNA and lipids is challenging. Therefore, incomplete understanding of pathomechanism contributes to missing therapeutic solutions. Neurons are highly polarized and display high morphological complexity. Potent and functional communication between their soma and distal processes (axons) is necessary for correct functioning [1]. Consequently, correct localization of mRNA and subsequent local protein synthesis is needed [2–5]. Interestingly, in neurodegenerative conditions like amyotrophic lateral sclerosis (ALS), Alzheimer's disease (AD), Huntington's disease (HD), glaucoma and hereditary spastic paraplegia (HSP), axonal degeneration often precedes and sometimes is causative of neuronal death [6–11]. Additionally, recent studies provide evidence that mRNAs are present in large quantities in the axon, implicating local translation as an important factor in axonal health and survival [12–14]. This in turn indicates that our understanding of local translation and its function needs revision and highlights the necessity for new methods decrypting the axonal transcriptome. Recent advances in stem cell research enable reprogramming of somatic cells into induced pluripotent stem cells (iPSCs) and their differentiation into different neuronal subtypes. This poses the chance to better understand homeostatic and disease conditions of the brain. Along this line, transcriptome profiling has been used as a valuable tool to investigate changes in the cell body and axonal protrusion of neurons derived from primary embryonic mouse motor neurons (MNs) and primary embryonic mouse dorsal root ganglia [15,16]. However, these datasets contained high numbers of proliferative and glial marker sets, suggesting contamination by other cellular components (CC) or non-neuronal cells [15,16]. More recently, Nijssen *et al*. developed an approach using a microfluidic device to clearly separate the axon from the cell body with sensitivity similar to single-cell sequencing [14], making it possible to closely examine the axonal transcriptome in healthy and diseased conditions.

To investigate transcripts and pathways critical for axonal maintenance and degeneration, we investigated kinesin family member 1C (*KIF1C*)-dependent changes to the axonal transcriptome. Mutations in *KIF1C*, a motor protein that is causative of an autosomal recessive form of HSP (SPG58, #611302), lead to axonal degeneration of central MNs. *KIF1C* is implicated in many functions, including maintenance of Golgi morphology, cell migration, formation of podosomes in vascular smooth muscle cells and macrophages and MHC presentation on the cell [17–23]. Interestingly, *KIF1C* has also been implicated in long-range directional transport of APC-dependent mRNAs and RNA-dependent transport of the exon junction complex (EJC) into neurites, suggesting *KIF1C* can bind RNA in a direct or indirect manner [24–26]. However, which impact loss of *KIF1C* has on the axonal transcriptome remains elusive.

Using microfluidic chambers, we here provide evidence that RNA-sequencing (RNA-seq) of axons of iPSC-derived cortical neurons (CNs) delivers high-quality, pure and reliable axonal transcriptome profiles. In agreement with previous studies, the axonal compartment contained only a subpopulation of genes compared to the soma and markers for glial and proliferative cells were absent. Importantly, we find that axons not only present with a distinct transcriptome that is clearly separated from the soma but also detected the presence of a set of RNAs coding for transcription factors (TF), previously unknown to be present in the axon.

We show that loss of *KIF1C* leads to widespread changes in this composition and unravels transcriptomic changes that may be relevant for other neurodegenerative diseases. Therefore, this study increases our understanding of homeostatic and disease-related transcriptome conditions in the soma and axons of iPSC-derived CNs.

## 2. Results

### 2.1. Microfluidic devices enable RNA-sequencing of induced pluripotent stem cell-derived human cortical neuron axons

To investigate changes in the axonal in relation to the somatic transcriptome in a human neuronal model, we performed RNA-seq on axonal and soma samples of iPSC-derived CNs that show characteristics of glutamatergic layer V and VI CNs. To demonstrate the purity of our iPSC-derived CN culture and ensure expression of cortical markers, immunocytochemical staining and real-time quantitative polymerase chain reaction (RT-qPCR) was performed (electronic supplementary material, figures S1 and S2). CN cultures formed complex networks and expressed neuronal markers (β-III-tubulin, TAU and MAP2) and markers of cortical layer V (CTIP2) and VI (TBR1; electronic supplementary material, figure S1A–C). Staining for the astrocytic marker glial fibrillary acidic protein (GFAP) was negative, indicating high purity of our culture (electronic supplementary material, figure S1D). No morphological differences were noted between wild-type (WT) and *KIF1C*-knockout (*KO*) CNs. RT-qPCR analysis revealed that iPSC-derived CNs expressed the cortical layer markers FoxG1 and PAX6, dendritic marker MAP2 and microtubule-associated marker DXC, while undifferentiated iPSCs were negative for these markers (electronic supplementary material, figure S2). Therefore, we conclude that a homogenous culture of neurons was generated that can be used as a cortical *in vitro* cell model. For RNA-seq, CNs were plated into microfluidic devices, and the axons were recruited to the empty chamber by using a gradient of glial cell line-derived neurotrophic factor (GDNF), brain-derived neurotrophic factor (BDNF) and nerve growth factor (NGF; electronic supplementary material, figure S3A,B). Subsequently, each compartment was individually lysed and subjected to RNA-seq (electronic supplementary material, figure S3A; see §5).

On average, each sample yielded 34.32 million pair-end reads, with a mean read length of 109 base pairs (bp). Quality assessments via MultiQC indicated that over 92% of these reads had a Phred score above 30 (Q30), pointing to high sequencing

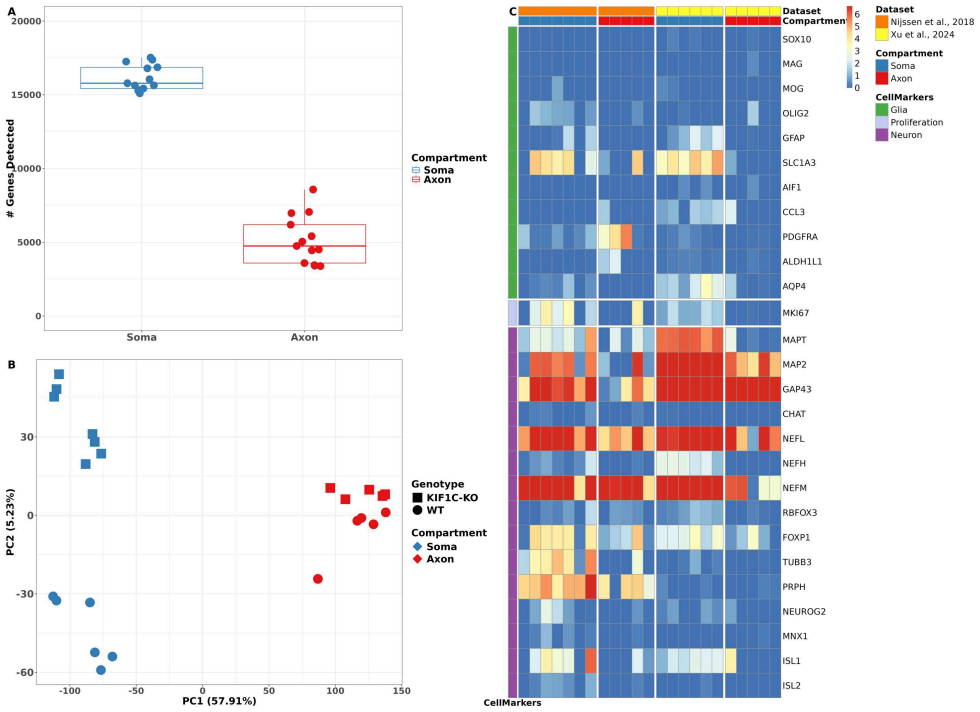


**Figure 1.** QC reveals RNA-seq for axonal compartments is highly specific. (A) Median number of gene counts detected in the soma (blue) and axonal compartment (red; TPM >1 in at least three samples; across all samples). The number of detected genes in the soma compartment (16 159 ± 880) is approximately threefold higher than in the axon compartment (5139 ± 1642). Data are presented as medium and interquartile range. (B) Post-QC PCA scatter plot. PC1 distinguishes the soma (blue) and axonal (red) compartment. PC2 distinguishes WT (circle) and *KIF1C*-KO (square) samples. (C) Expression $\log_2$(TPM) values of glial (green, top row), proliferative (lavender, middle row) and neuronal marker genes (purple, bottom row) in soma (blue, left columns) and axonal compartments (red, right columns), in the Nijssen et al. [14] dataset (orange, left) and our dataset (this dataset; yellow, right). As in the samples from Nijssen *et al.*, our samples show low expression of glial and proliferative marker genes while neural marker genes are highly expressed.

fidelity. We aligned these fastq reads to reference the genome using STAR, achieving an average mapping rate of 89.1%. Following alignment, gene expression was measured in transcripts per million (TPM) values via featureCounts.

In total, 20 199 genes were detectable across all datasets, with a TPM >1 in at least three RNA samples. Among the whole dataset, the soma samples exhibited an average of 16 159 ± 880 detectable genes, whereas the axon samples demonstrated a significantly lower count, with an average of 5139 ± 1642 genes (figure 1A). An initial principal component analysis (PCA) highlighted sequencing batch effects, which were corrected using the ComBat method from the preprocessCore package. Three axon RNA-seq samples (two WT and one *KIF1C*-KO sample) were removed due to their poor correlation ($r < 0.5$) with other samples. The remaining samples passing the final quality control (QC) resulted in 13 soma (WT: 6; *KIF1C-KO*: 7) and 10 axonal samples (WT: 5; *KIF1C-KO*: 5; electronic supplementary material, figure S4 and table S1).

The final PCA after batch correction and sample QC illustrated distinct clustering (figure 1B). Principal component (PC) 1 prominently differentiated the transcriptome of the axon from soma samples, emphasizing their considerable transcriptional disparities. Concurrently, PC2 separated samples by genetic background—WT versus *KIF1C-KO* (figure 1B).

To confirm our samples' cellular composition and purity, we referred to a list of recognized glial, neuronal and proliferative marker genes (electronic supplementary material, table S2) and visualized their expression in a heatmap (figure 1C). The analysis revealed that our RNA-seq samples, which passed QC, exhibited strong expression of neuronal markers while showing a marked absence of glial or proliferative marker expression (figure 1C). Comparison of our data to a recently published dataset, focusing on human stem cell-derived spinal motor axons [14], revealed a congruent expression pattern (figure 1C).

In summary, we demonstrate that our experimental paradigm, which uses microfluidic devices to separate neuronal axons from soma, enables RNA-seq of axonal fractions with a high specificity. Intensive QC revealed high purity of both compartments without contamination by either glial components or cell somas in the axonal compartment.

## 2.2. Axonal compartments of induced pluripotent stem cell-derived cortical neurons show a unique transcriptional RNA profile

Next, we aimed to delineate the transcriptomic differences between soma and axonal compartments. For this, we analysed five WT axon and six WT soma samples. On average, we detected 16 207 ± 981 expressed genes (TPM >1) in WT soma samples and 5075 ± 2080 genes (TPM >1) in axon samples. Of note, we detected a slightly higher number of genes in both compartments compared to two recently published datasets, investigating human-derived lower MNs or i3 neurons (electronic supplementary material, figure S5) [14,27], using similar cultivation techniques. In contrast, a significantly higher number of genes detected in the axonal compartment was described by a paper using different cultivation, lysis and sequencing techniques [28]. Comparing genes detected in the axonal compartment of human-derived CNs to previously published sequencing data of mouse-derived

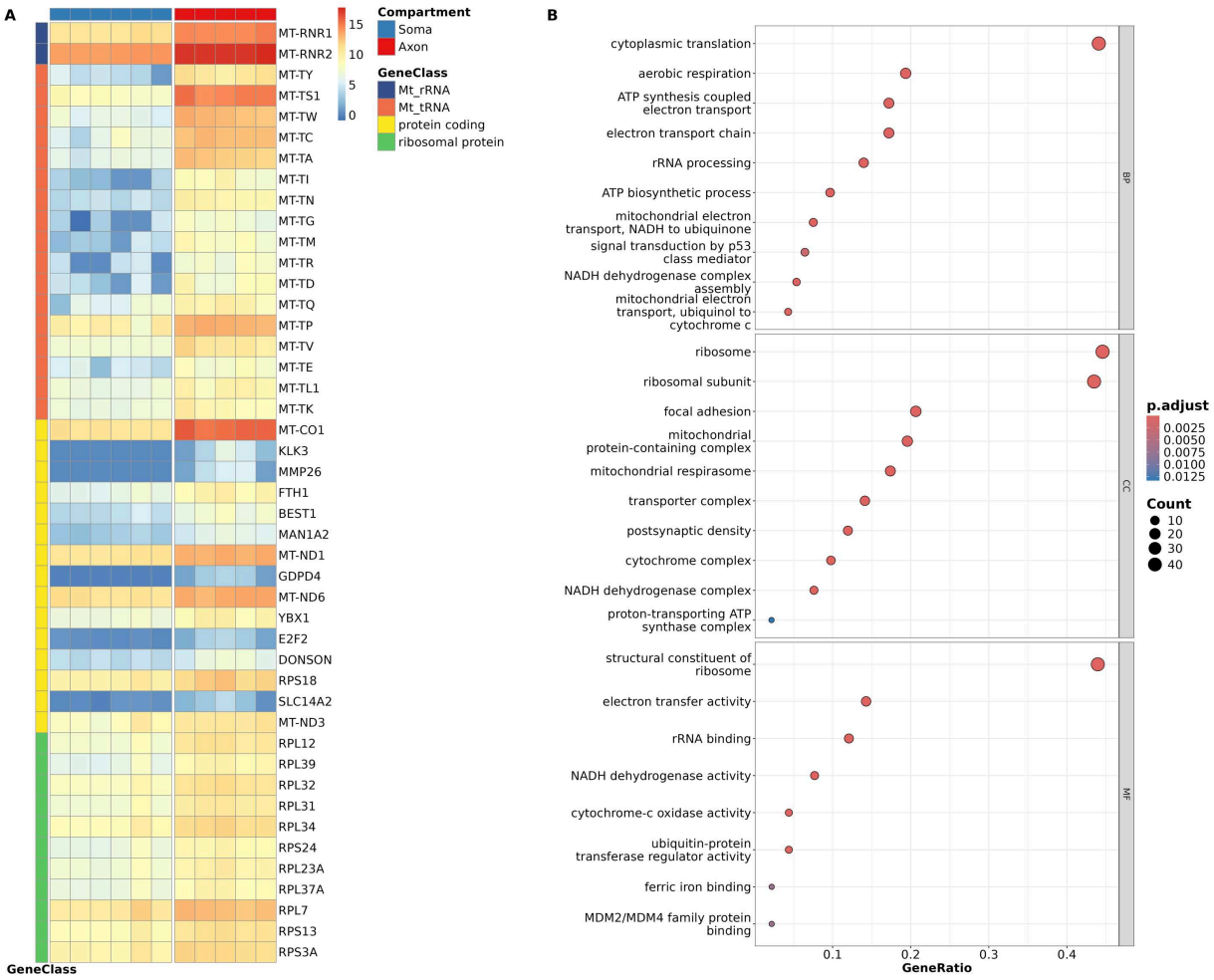


**Figure 2.** Axonal transcriptome of WT CNs is distinct from the soma transcriptome. (A) Expression ($log_2$(TPM)) of top genes that are higher expressed in the axonal (red, right column) compared to the soma compartment (blue, left column; adjusted *p*-value < 0.05, logFC > 2). Genes are grouped by gene class (purple: mitochondrial (Mt)_rRNA; orange: Mt_tRNA; yellow: protein coding; green: RP). (B) GO term enrichment analysis of axon-enriched genes connected to protein coding or RP genes primarily spotlighted mitochondrial processes and ribosome processes functions. BP, biological process; CC, cellular component; MF, molecular function.

MNs [14,16], we only detected little overlap between the datasets (electronic supplementary material, figure S6), emphasizing the need for human-derived cell models in translational research.

Interestingly, the analysis of the top 100 expressed genes within each compartment demonstrated that 57 genes exhibited compartment-specific expression, and the profile of highly expressed genes varied between compartments: in the soma, we predominantly detected protein-coding mRNAs, with diverse functional implications, whereas axonal expression was characterized by a broader spectrum of gene classes, including a notable prevalence of RNAs encoding ribosomal proteins (RP genes) and mitochondrially encoded RNAs (electronic supplementary material, figure S7A,C). Of note, 43 of the top overall 100 genes were concurrently expressed in both axon and soma, demonstrating a significant convergence (electronic supplementary material, figure S4B). Among these, two genes encoding microtubule-associated proteins, Stathmin (*STMN)1* and *STMN2*, were identified. These proteins are pivotal in axonal development and repair [29–31]. Furthermore, we detected *GAP43*, which plays a significant role in axonal growth, particularly during development and regeneration [32,33].

Genes with expression levels of TPM >1 in a minimum of three samples in axon and soma were considered for studying transcriptomic differences. Differential expression analysis identified 14 056 genes differentially expressed (false positive discovery rate (FDR)-adjusted *p*-value < 0.05) between the compartments: 13 745 genes were enriched in the soma compared to the axon, and 311 were enriched in the axon compared to the soma (electronic supplementary material, figure S8). PCA, considering all expressed genes in WT compartments, distinctly separated the axon from the soma, with PC1 accounting for 68.3% of the variance (figure 1B), underscoring the distinct transcriptomic profile of the axonal compartment. Interestingly, the most significantly enriched genes in the axon, displaying a logFC >2 and an adjusted *p*-value < 0.05, were involved in ribosomal subunits (e.g. *RPL12, RPL39* and *RPL31*), respiratory chain complex (e.g. *MT-ND1* and *MT-CO1*), ion transport (e.g. *BEST1*) and mRNA splicing (e.g. *YBX1*; figure 2A). Consequently, Gene Ontology (GO)-term analysis of axon-enriched genes primarily spotlighted ribosome process functions and mitochondrial processes (figure 2B).

## 2.3. Axons of induced pluripotent stem cell-derived cortical neurons show a unique transcription factor profile

Recent studies have highlighted that TF mRNAs present in axons can be translated, undergo retrograde transport and alter gene transcription [34–39]. To explore this further, we evaluated expression of a diverse range of TF mRNAs from various organisms

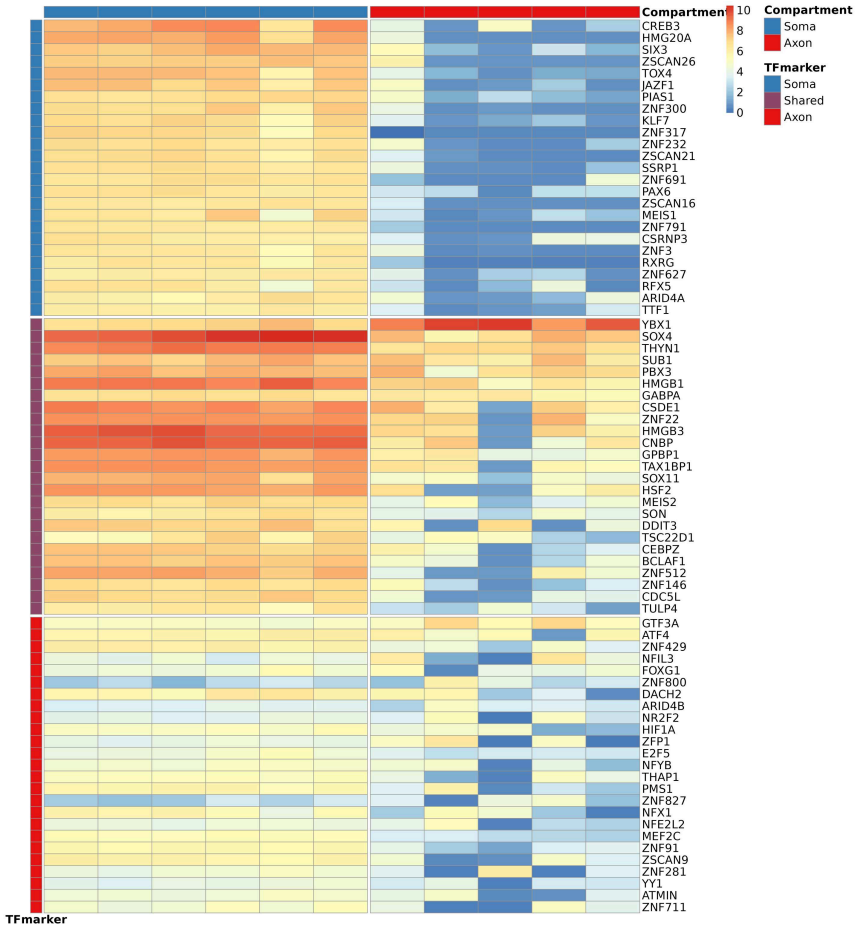


**Figure 3.** Axon and soma present with specific TF mRNAs. Top expressed TF mRNAs in the soma compartment (blue, top row), shared compartment (purple, middle row) and axon compartment (red, bottom row) and expression in soma (blue, left column) and axon compartment (red, right column) of iPSC-derived WT CNs. *CREB3* is the top expressed in the soma compartment, while *YBX1*, *SOX4*, *SUB1* and *THYN1* are shared between axon and soma, and *GTF3A* is top expressed in the axon compartment.

in our WT dataset [40]. Upon analysing the top 50 expressed TF mRNAs separately in axons and somas, we discovered a shared set of 25 TF mRNAs between the two compartments, including key factors like *YBX1*, *SOX4*, *THYN1* and *SUB1* (figure 3). In addition to these shared TF mRNAs, each compartment exhibited 25 unique top expressed TF mRNAs, highlighting the specificity of their transcriptional landscapes. Specifically, *GTF3A* and *ATF4* were identified as the leading axonal TF mRNAs, both well-known for their roles in the nucleus initiating transcription [41,42] (figure 3). Moreover, *CREB3* emerged as the most prominent TF mRNA in the soma, playing a crucial role in myelination and axonal growth (figure 3) [43,44].

## 2.4. Kinesin family member 1C modulates the axonal transcriptome

*KIF1C* deficiency causes HSP, a disorder associated with prominent length-dependent degeneration of central MN axons. As *KIF1C* has recently been implicated in long-range transport of mRNAs and the EJC [24–26], we studied the axonal transcriptome of *KIF1C-KO* iPSC-derived CNs to highlight transcripts and pathways essential for MN degeneration and maintenance. We did not see gross abnormalities in neuron differentiation, axon growth or axon length in *KIF1C-KO* compared to control CNs. As hypothesized, both axonal and soma compartments in the *KIF1C-KO* cells exhibited markedly reduced *KIF1C* expression when compared with WT compartments (figure 4A). Looking at the total gene counts, *KIF1C-KO* axons exhibited expression of 5099 ± 1642 genes, while WT axon samples displayed 5075 ± 2080 genes. In the soma, we detected 16207 ± 981 genes in *KIF1C-KO* CNs and 16118 ± 862 in the WT (electronic supplementary material, table S3). For differential expression analysis, we included genes with a TPM >1 in at least three samples across combined conditions. Ablation of *KIF1C* resulted in a statistically significant differential expression ($p$-value < 0.001) of 189 genes within the axon compared to WT axons (electronic supplementary material, figure S9). Intriguingly, this dysregulation was specific to the axon, as only 12 of these also displayed dysregulation in the soma of *KIF1C-KO* CNs (electronic supplementary material, figure S8A,B). *PAX6*, *VIM*, *LGALS1*, *CCND2*, *MIR9-1HG*, *GPR26*, *NR2F2* and *LAMTOR5-AS1* were downregulated in both axon and soma of *KIF1C-KO* CNs compared to WT, and *ZIC2*, *GNRH1*, *GNG8* and *NOL4L* were upregulated in both compartments. In total, 89 genes showed decreased expression in the axon of *KIF1C-KO* CNs, while the remaining 100 exhibited increased expression (electronic supplementary material, figure S9A,B). Furthermore, 21 of the 89 downregulated genes were protein coding and were totally absent in *KIF1C-KO* CNs (figure 4C).

Among the transcripts absent or severely downregulated in *KIF1C-KO* CN axons are several key transcripts critical for neuronal and axonal functions (figure 4C). These transcripts include *ESYT2*, known to play a role in synaptic growth and neurotransmission, *LGI2*, involved in inhibitory synapse assembly [45,46], *NAB1*, a transcriptional repressor with a role in

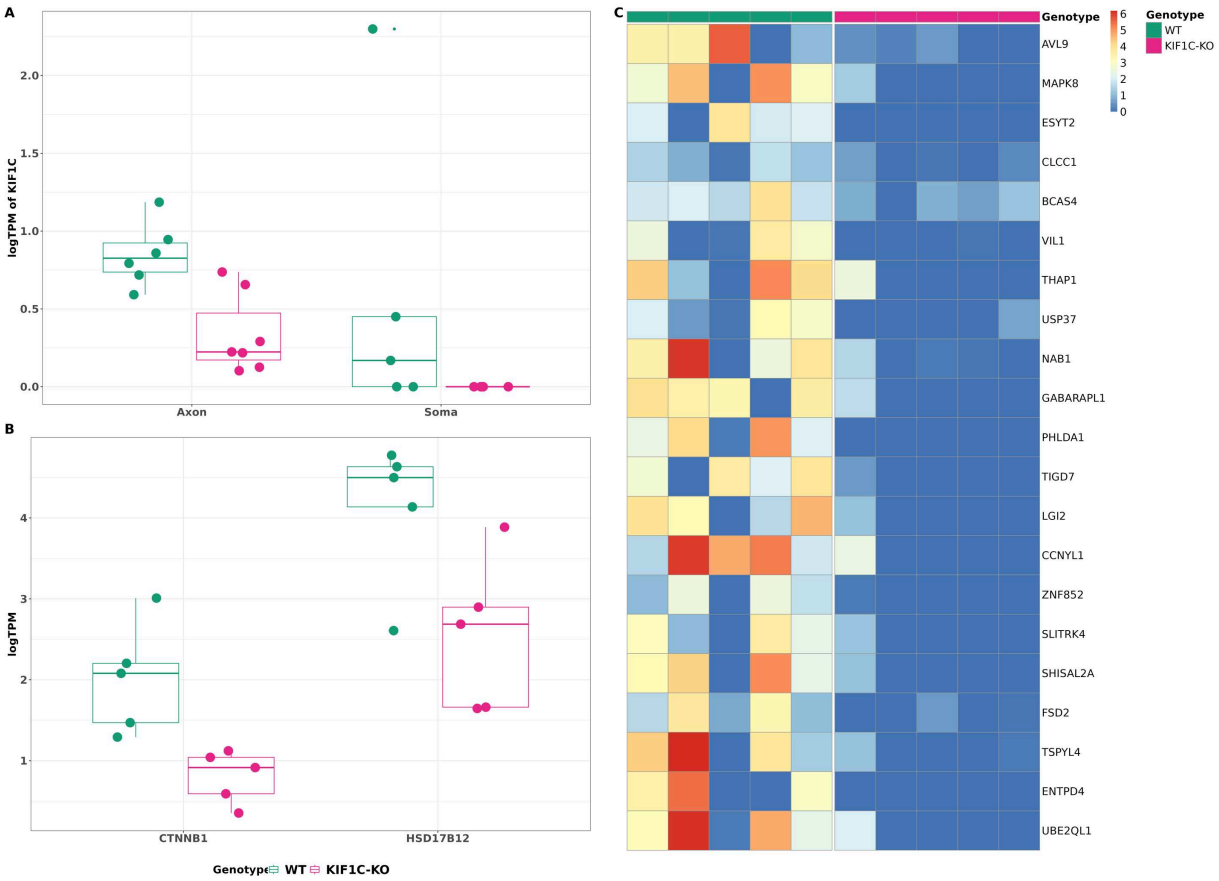


**Figure 4.** *KIF1C* modulates the axonal transcriptome. (A) *KIF1C* expression is reduced in the axon and soma compartments of *KIF1C-KO* (magenta) compared to WT CNs (teal). Data are presented as medium and interquartile range. (B) Two APC-target genes show decreased expression in the axons of *KIF1C-KO* compared to WT CNs (WT: teal, KIF1C-KO: magenta). Data are presented as medium and interquartile range. (C) Heatmap of protein coding that are absent in axons of *KIF1C-KO* compared to WT CNs. All indicated genes are differentially expressed between WT and *KIF1C-KO* axons ($p$-value < 0.001).

**Table 1.** Pathways or gene sets curated for downregulated genes in *KIF1C-KO* axon connected to axon guidance or development.

| dysregulation | gene | geneset or pathway |
|---|---|---|
| downregulated | *PPP3CB* | KEGG_AXON_GUIDANCE GOBP_AXON_DEVELOPMENT |
| downregulated | *SLITRK4, PAX6* | GOBP_AXON_DEVELOPMENT |
| downregulated | *CLCN3* | GOCC_AXON, GOCC_DISTAL_AXON |
| downregulated | *MAPK8* | GOCC_AXON |

synaptic active zone assembly [47,48], *PHLDA1*, involved in injury response [49], *CLCC1*, involved in misfolded protein clearance [50], *THAP1*, implicated in dystonia (DYT6, # 602629) [51], and *SLITRK4*, involved in controlling excitatory and inhibitory synapse formation [52]. Additionally, a sub-group of the downregulated genes in the axons of *KIF1C-KO* CNs appear to be involved in axonal pathways. For example, *PPP3CB* is catalogued under KEGG's axon guidance pathway, while *SLITRK4*, *PAX6*, *MAPK8* and *CLCN3* are enshrined within the GO term's axon-related gene set (table 1).

It has been previously described that *KIF1C* plays a role in localizing APC-target mRNAs to cytoplasmic protrusion [53]. However, only two known targets of APC, *CTNNB1* and *HSD17B12*, were specifically downregulated in axons of *KIF1C-KO* CNs (figure 4C).

Taken together, these data show that *KIF1C* plays an important role in the axonal and soma transcriptome, and loss of *KIF1C* in CNs leads to widespread transcriptional changes with implications in critical neuronal and axonal functions.

## 3. Discussion

Axonal RNA biology is increasingly implicated in the healthy and diseased CNS. Here, we generated high-quality and pure axonal transcriptomes from iPSC-derived CNs, using a previously developed RNA-seq approach [14] with adaptations, and careful application of bioinformatic QC. Our axon samples showed significantly fewer genes than previous datasets from mouse- or human-derived axons [16,28,54], which were probably contaminated by non-neuronal cells or somata. Interestingly, our results align with recent, highly specific datasets [14,27], though we observed slightly higher gene numbers likely due to our

improved lysis protocol, longer paired-end reads and deeper sequencing. Importantly, our data lacked glial and proliferative markers, indicating highly specific neuronal and axonal cultures. When comparing our data to previously published datasets using mouse-derived cells [14,16], we found only little overlap of axonal genes, emphasizing the necessity for human-specific research to achieve translational relevance.

Earlier work on human-derived cells focused on axonal transcripts in specific disease contexts, such as ALS in lower MNs [14] and lysosomal-dependent transport in the context of Parkinson's disease (PD), AD, HD or ALS using i3 neurons [27]. In contrast, our work provides a broader overview of molecular profiles in iPSC-derived CNs and explores a previously uncharacterized disease context. Unlike lower MNs, residing in the peripheral nervous system, and i3 neurons, which resemble cortical-like neurons but do not fully recapitulate all aspects of CNS-resident neurons, our study focuses on human-derived CNS-resident CNs. Thus, this study offers a broad analysis of axonal and neuronal transcripts relevant to neurodegenerative diseases. Our specific harvesting and sequencing techniques enabled us to identify transcriptional differences impacting general neuronal function and pathology.

Our comprehensive transcriptomic analysis revealed distinct transcriptional landscapes in the axon and soma compartments. While most detected genes specific to the soma compartment represent protein-coding mRNAs, involved in functions essential for neuronal survival and maintenance, axonal compartments showed a more variable range of gene types, including protein-coding mRNAs, RNAs encoding RPs, mitochondrial-encoded RNAs and long non-coding RNAs (lncRNAs). Recent work has provided evidence that local translation of mRNAs in the axons plays an important role in neuronal development, function, plasticity and disease [55]. Local translation is regulated by various mechanisms: binding of extrinsic cues to their receptors on the cell surface of axons can trigger local translation [56], or chemical signalling through specific cues can activate kinases and phosphorylate RNA-binding-proteins resulting in mRNA translation [57]. Interestingly, extrinsic cues like growth factors and nutrients have been shown to activate mTOR signalling, which in turn increases translation of axonal mRNAs [58,59]. Previous studies have shown that RNAs encoding RPs are enriched in mammalian axons, mouse and *Xenopus* growth cones, rat hippocampal dendrites and *Aplysia* neurites [12,13,60–64]. Similarly, we detected RNAs encoding for RPs in axons of CNs. While their function remains largely unknown, it is possible that they may be involved in ribosomal repair or renewal of components in already assembled ribosomes [65]. Strengthening this hypothesis, it has been shown that mRNAs encoding RPs are present and locally translated in axons and can be incorporated into axonal ribosomes in a nucleolus-independent manner [66]. Of note, we detected the presence of lncRNAs in the axonal compartment. Recently, a lncRNA has been found to be actively involved in local axonal translation [67], suggesting that lncRNAs in axons have specific functions. The distinct mRNA profile in axons, including nuclear-encoded transcripts related to ribosomal subunits, respiratory chain complex, ion transport and mRNA splicing genes, emphasizes the unique metabolic and synthetic demands of this compartment. This aligns with the hypothesis that axons, despite their dependence on the soma, maintain a degree of autonomy in protein synthesis and energy production, which may be crucial for their function and health.

Transcripts found in both compartments were largely consisting of mitochondrially encoded genes related to NADH metabolism (e.g. *MT-ND1,2,4* and *NDUFA1*), the mitochondrial respiratory chain (e.g. *MT-CO1–3* and *MT-CYB*) or mitochondrial ribosomal functions (e.g. *MT-RNR1&2* and *RPL12*). The rest of the shared signatures were related to cytoskeletal or microtubule organization (*TMSB10, STMN1, STMN2* and *TUBA1A*) and homeostasis/signalling pathways (e.g. *FTL, GAPDH* and *DAD1*). These signatures likely reflect the high energy and organizational demands of axon and soma. Interestingly, only one shared gene was related to neurite formation, axon growth, regeneration and plasticity (*GAP43*) [33]. While the role of *GAP43* in the soma is well described, more recently, axonal protein synthesis of *GAP43* was shown to promote axon growth [33,68].

Recent work has shown that TF mRNAs are not only involved in defining neuronal identity in early development and during survival but also function outside the soma. They can be locally synthesized and retrogradely transported back to the nucleus, where they can influence gene transcription and be involved in plasticity, axon pathfinding and neuroprotection [34–37,69–72]. Therefore, we performed in-depth analysis of enriched TF mRNAs specific to either compartment or common between them. We found that highly expressed TF mRNAs in the soma were related to neural differentiation, morphogenesis, maturation and survival. Of note, two TF mRNAs have been found to be involved in myelination and axonal growth (*RXRG* and *CREB3* [43,44,73]), probably reflecting the ongoing growth of axons *in vitro*. In contrast, many TF mRNAs detected in the axonal compartment were related to axon guidance and/or axonal/neuronal regeneration. This is not surprising as several studies have demonstrated that local translation in axons can promote cytoskeletal and membranous growth [74–76]. We further detected *YBX1* in the axon and soma. *Ybx1* has been found to be enriched specifically in distal motor axons of mice [14]. *YBX1* plays an important role in binding and stabilizing cytoplasmic mRNAs, regulating translation and mediating anterograde axonal transport [77,78]. Therefore, it is plausible that it can act as an important mediator between axon and soma. Additionally, we found *GTF3A* and *ATF4* enriched in the axonal compartment. These TFs are traditionally linked to transcription initiation and stress response in the nucleus [41,42]. Importantly, *ATF4* has previously been shown to be locally synthesized in the axon and retrogradely transported to the soma [79–81], suggesting that other TF mRNAs traditionally viewed as nuclear may be, too. In line with this, we detected a substantial number of TF mRNAs with unknown (e.g. *ZNF429*, *ZNF800* and *ZSCAN9*) or nucleus-related functions, like transcription, cell cycle progression and cell proliferation (e.g. *ATMIN*, *NFX1*, *THAP1*, *E2F5* and *NR2F2*) in the axon. The discovery of these TF mRNAs signifies a major advancement in our understanding of the molecular mechanisms underpinning axonal functions. These findings not only challenge conventional views of axons as mere passive conduits but also highlight their role as active sites of complex regulatory activities. The potential intra-axonal translation and retrograde transport of translated TFs unveils a dynamic aspect of axons, where they adaptively respond to both internal and external stimuli. This novel paradigm in neuronal biology raises critical questions about the functional roles of TFs within axonal compartments, diverging from their established nuclear functions.

To further investigate changes of the axonal compartment in diseased conditions and thus gain an understanding of axonal transcripts essential for axon maintenance, we investigated *KIF1C-KO* CNs. *KIF1C*, a kinesin family member, is implicated in HSP, a group of heterogeneous genetic disorder resulting in degeneration of upper MN axons [82–87]. Indeed, loss of *KIF1C* led to widespread changes of the transcriptome, showing axon-specific effects. This may be explained, as *KIF1C* is the fastest human cargo transporter and is implicated in long-range and highly dynamic transport [88]. It has long been appreciated that axonal transport is important for survival and health of neurons, and disturbance in axonal transport is a key pathological event that contributes to diverse neurodegenerative diseases like AD, polyglutamine diseases, HSPs, ALS, PD and Charcot–Marie–Tooth disease [89,90]. Additionally, mutations in motor proteins like *KIF5A*, dynein and dynactin have been shown to cause neurodegeneration [91–95], strongly supporting the view that defective axonal transport can directly trigger neurodegeneration. Therefore, spatial dysregulation of transcription due to *KIF1C* loss may uncover transcriptional changes also relevant in other neurodegenerative diseases.

*KIF1C* has previously been shown to transport APC-dependent mRNAs to cell protrusion, and it is implicated in the transport of the EJC in neuronal SH-SY5Y cells [24,25]. Therefore, it is not surprising that we see the near complete absence of several key transcripts critical for neuronal and axonal function in axons of *KIF1C-KO* CNs. Interestingly, even though *KIF1C* has been shown to transport mRNAs in an APC-dependent manner, only a subset of the detected missing factors was connected to APC-dependent transport. One explanation for this may be that different motors can be used in different cell types: the transport of $\beta$-actin mRNA, which accumulates at the leading edge of migrating cells, involves several motors that display cell type and compartment specificity, differing between neurons and fibroblasts [96–104]. Interestingly, in mouse fibroblasts, APC-dependent RNAs were involved in pathways functionally relevant to cell movement [105]. However, in this study, genes related to APC-dependent transport did not display functional relevance for movement. Instead, most downregulated RNAs in *KIF1C-KO* axons were related to neurotransmission, the synaptic zone and misfolded protein clearance. Since the previously mentioned investigations regarding *KIF1C* have been performed in other cell types [24–26,105], it is possible that *KIF1C*-dependent transport in CNs uses different motors, independent of APC. However, by which mechanism transport in CNs is conducted needs to be subject of future investigations. Our study has certain limitations, notably the absence of validation of key transcripts in *KIF1C-KO* CNs. Future research should address these limitations to provide a more comprehensive mechanistic understanding.

Taken together, our findings regarding *KIF1C* provide novel insights into the role of motor proteins in axonal transcriptome modulation. Importantly, genes and TFs dysregulated due to *KIF1C* loss may also be implicated in other neurodegenerative diseases.

## 4. Conclusion

Collectively, our study not only affirms the transcriptional distinctiveness of axonal and soma compartments in iPSC-derived CNs but also sheds light on the intricate molecular machinery governing these compartments. The identification of not only compartment-specific gene expression patterns but also compartment-specific TF mRNAs, as well as the role of *KIF1C* in modulating these, have significant implications for our understanding of neuronal biology and the pathophysiology of MN diseases. Future research focusing on the functional implications of these transcriptional differences and the potential of targeting specific pathways within axons could pave the way for novel therapeutic approaches in neurodegenerative diseases.

## 5. Methods

### 5.1. Differentiation of induced pluripotent stem cells to cortical neurons

Human iPSCs were approved for use by the Institutional Review Boards, University of Tübingen Medical School, Germany (approval number: 423/2019BO1). The *KIF1C-KO* line (homozygous KO [106]) and isogenic control line were grown in essential 8 (E8) medium on diluted Matrigel solution (1 : 60, Corning) coated six-well plates at 37°C, 5% $CO_2$ and 100% relative humidity. Medium was changed daily. Cells were differentiated into CNs of layers V and VI. The differentiation followed previously established protocols [106–108]. Briefly, iPSCs were seeded at a density of $3 \times 10^5$ cells $cm^{-2}$ on Matrigel-coated plates (Corning), in E8 medium supplemented with 10 µM SB431542 (Sigma-Aldrich) and 500 nM LDN-193189 (Sigma-Aldrich). The cells underwent neural induction over 9 days. Post-induction, on day 9, the cells were split at a 1 : 3 ratio and then cultured in 3N medium with 20 ng $ml^{-1}$ FGF-2 for an additional 2 days. From day 11 to day 26 after induction (DAI 11–26), cells were maintained in 3N medium, with medium changes occurring bi-daily. On DAI 26, the cells were transferred to microfluidic chambers (XC950, Xona Microfluidics) for cultivation.

### 5.2. Immunocytochemistry

Characterization of CNs was performed by immunostaining. Neuronal markers (β-III-tubulin and TAU), markers of the cortical layer V (CTIP2) and IV (TBR1) and a dendritic marker (MAP2) were used for characterization (table 2). Additionally, the astrocyte marker GFAP was used to ensure culture purity (table 2). On DAI37, CNs were washed twice with phosphate-buffered saline (PBS) and fixed using 4% (w/v) paraformaldehyde (Merck) for 15 min at room temperature (RT). Following, cells were washed three times with PBS and incubated with 5% BSA in 0.1% Triton X/PBS (PBS-T) or 10% NGS in 0.3% PBS-T for

**Table 2.** Antibodies, dilution, and corresponding blocking solution/dilutant used for characterization of iCNs.

| primary antibody | dilution | blocking |
|---|---|---|
| β-III-tubulin (Sigma-Aldrich, T8660) | 1 : 750 | 5% BSA/0.1% Triton X/PBS |
| CTIP2 (Abcam, ab18465) | 1 : 500 | 5% BSA/0.1% Triton X/PBS |
| MAP2 (Proteintech, 17490-1-AP) | 1 : 250 | 5% BSA/0.1% Triton X/PBS |
| TAU (CST, #46687) | 1 : 1000 | 5% BSA/0.1% Triton X/PBS |
| GFAP (CST, CSIG 80788T) | 1 : 200 | 5% BSA/0.1% Triton X/PBS |
| TBR1 (Proteintech, 2093-1-AP) | 1 : 200 | 10% NGS/0.3% Triton X/PBS |

1 h at RT (table 2). The primary antibodies in blocking solution were applied and incubated at 4°C overnight. After washing three times with PBS-T, the secondary antibody (AF488 (Thermo Fisher Scientific, A11001) or AF568 (Thermo Fisher Scientific, A11004)), diluted in blocking solution, was applied for 1 h at RT in the dark. For nuclear staining, cells were washed three times with PBS-T and incubated with DAPI (1 : 10 000; Thermo Fisher Scientific, 62248) for 5 min at RT. The coverslips were mounted with fluorescence mounting solution (DAKO; Agilent, S3023) on objective slides. Images were acquired using a Zeiss inverted fluorescence microscope Axio Observer 7.

## 5.3. Real-time quantitative polymerase chain reaction analysis

RNA of CNs was reverse transcribed using the Transcriptor High Fidelity cDNA Synthesis Kit (Roche) following the manufacturer's instructions. Briefly, 500 ng RNA was reverse transcribed to cDNA by incubating the RNA with random hexamer primers for 10 min at 65°C followed by reverse transcription with the Transcriptor High Fidelity Reverse Transcriptase. RT-qPCR was performed to characterize CNs. cDNA (1 : 10) was mixed with Light Cycler 480 SYBR Green I Master (Roche) and the respective qPCR primers (10 µM) for the housekeeping gene GAPDH and for the dendritic marker MAP2, cortical markers FoxG1 and Pax and microtubule-associated marker DCX. Transcription level quantification was performed on a LightCycler 480 with a touch down qPCR program in three technical replicates. Expression level quantification was carried out with LightCycler 480 software tool 'relative quantification' by normalizing CP values to the housekeeping gene. Undifferentiated iPSCs were used as a negative control for cortical markers.

## 5.4. Culturing of cortical neurons in microfluidic devices

Microfluidic devices were set-up following the procedure outlined by Nijssen *et al.* [14] with modifications regarding the cultivation and lysis protocol (electronic supplementary material, figure S3). Briefly, both compartments of the device were precoated with XC Pre-Coat (Xona Microfluidics), with one compartment receiving a 1 min incubation and the other a 5 min incubation. Following the coating, the chambers were washed twice with PBS, coated with polyornithine, incubated at RT for 1 h and subsequently coated with a diluted Matrigel solution (1 : 45; Corning), followed by a 1 h incubation at 37°C. After two washes with 3N Medium, the compartments were filled with 3N Medium supplemented with Rock inhibitor (RI, 1 : 1000) and maintained at 37°C until neuron loading. DAI26 neurons were washed with PBS, incubated with Accutase + RI for 20 min at 37°C, strained through a 70 µm cell strainer and suspended in 5.5 ml 3N + RI medium. A total of $2 \times 10^5$ neurons were loaded into each microfluidic chamber. The next day, 10 µM PD0325901 (Tocris) and 10 µM DAPT (Sigma-Aldrich) were added to the soma compartment. Cells were kept in this media for 4 days with media change every 2 days, followed by incubation with 3N media. In total, 10 ng $ml^{-1}$ of NGF, BDNF and GDNF were added to the axonal compartment to attract axons. Media changes were implemented three times per week, and fluid volumes were adjusted to ensure cross-chamber flow and to establish a trophic factor gradient from axonal to somatic compartments. Of note, the soma compartment contains not only cell bodies but also corresponding axonal fractions. For simplicity purposes, we will refer to this compartment as soma compartment throughout this paper.

## 5.5. Harvesting

At DAI 58, the RNA was extracted (electronic supplementary material, figure S3). DAI 58 was chosen for harvesting, because the axonal chamber was adequately overgrown to ensure a high RNA yield for the sequencing approach. No gross morphological differences between WT and *KIF1C-KO* neurons were observed at this time point. The compartments were washed with PBS. For the axonal compartment, 5 µl of NEBNext Cell Lysis Buffer (NEB, Massachusetts, US) was added directly into the corresponding microgroove. After 3 min, the solution was mixed and snap-frozen on dry ice. The soma compartment was lysed using 50 µl RLT buffer (Qiagen, Venlo, Netherlands) and then collected and snap-frozen using dry ice. Soma RNA was purified using the RNeasy Mini Kit (Qiagen, Venlo, Netherlands) following the manufacturer's instructions.

## 5.6. RNA-sequencing library construction

Due to the low amount of RNA available in the axon fraction, lysate from approximately 500 cells was prepared in 5 µl of NEBNext Cell Lysis Buffer and used for library preparation with the NEBNext Single Cell/Low Input RNA Library Prep Kit,

following the protocol for low-input cells. The library molarity was determined by measuring the library size (approx. 330 bp) using the Fragment Analyzer 5300 and the Fragment Analyzer DNA HS NGS fragment kit (Agilent Technologies) and the library concentration (>2 ng $\mu l^{-1}$) using Qubit Fluorometric Quantitation and dsDNA high sensitivity assay (Thermo Fisher Scientific). The libraries were denaturated according to the manufacturer's instructions, diluted to 270 pM and sequenced as paired-end 100 bp reads on an Illumina NovaSeq 6000 (Illumina). The sequencing aimed to achieve a depth of >15 million clusters per sample.

### 5.7. Short reads RNA-sequencing processing and differential gene expression analysis

Our RNA-seq pipeline encompassed read QC, RNA-seq mapping and gene quantification. Raw RNA-seq data were processed using the megSAP pipeline, which includes QC and adapter removal of fastq files. The reads were then aligned to the reference genome using STAR (v. 2.7.10a) [109]. Gene and transcript expression quantification was performed using featureCounts (subread-2.0.2) [110]. Transcript and gene abundances were expressed as TPM values.

To identify differentially expressed genes between soma and axon compartments of control lines, we first filtered out lowly expressed genes by keeping only those with at least 1 TPM value in at least three samples in each compartment. The filtered TPM matrix was taken as a $\log_2$ transformation. Differential expression analysis was performed using the Limma-Voom module. For the enrichment analysis of GO terms, we utilized the ReactomePA package in R (v. 4.3). This analysis encompassed the evaluation of significantly enriched pathways within the categories of biological processes (BP), CC and molecular functions (MF). The most significantly enriched pathways were meticulously assessed, and the top distinguished functional pathways were selected for visualization.

To compare our data with previously published datasets, we implemented the following procedures: for the dataset by Nijssen *et al*. [14], we first converted their counts per million values to TPM values. Subsequently, we required at least two WT samples for both soma and axon to have TPM values greater than 1. For the datasets of De Pace *et al*. [27] and Maciel *et al*. [28], which contained only two and three WT soma and axon samples in each dataset, we similarly converted the data to TPM values and included genes with TPM values greater than 1 in both samples.

Ethics. The use of human iPSCs in this study was approved by the Institutional Review Boards of the University of Tübingen Medical School, Germany (approval number: 423/2019BO1). Informed consent was obtained from all participants prior to sample collection.

Data accessibility. Due to ethical, legal and GDPR-related restrictions concerning human-derived samples, the raw sequencing data cannot be made publicly available. Researchers may request access to the dataset by contacting the corresponding author (R.S.). Access will be granted on a case-by-case basis, subject to institutional approvals and completion of appropriate data access agreements.

Supplementary material is available online [111].

Declaration of AI use. We have not used AI-assisted technologies in creating this article.

Authors' contributions. J.X.: conceptualization, formal analysis, investigation, methodology, software, validation, visualization, writing—original draft, writing—review and editing; M.H.: conceptualization, data curation, formal analysis, investigation, methodology, supervision, validation, visualization, writing—original draft, writing—review and editing; M.Na.: conceptualization, investigation, methodology, writing—review and editing; P.P.: investigation, methodology, writing—review and editing; M.K.: investigation, methodology, writing—review and editing; M.No.: investigation, writing—review and editing; S.H.: conceptualization, funding acquisition, methodology, writing—review and editing; L.S.: conceptualization, funding acquisition, methodology, writing—review and editing; J.A.: formal analysis, investigation, methodology, software, writing—review and editing; N.C.: formal analysis, investigation, methodology, software, writing—review and editing; R.S.: conceptualization, data curation, formal analysis, funding acquisition, investigation, methodology, project administration, resources, software, supervision, validation, visualization, writing—original draft.

All authors gave final approval for publication and agreed to be held accountable for the work performed therein.

Conflict of interests. We declare we have no competing interests.

Funding. This work was funded by the Bundesministerium für Bildung und Forschung (BMBF) through funding for the TreatHSP network (grants 01GM1905A and 01GM2209A to R.S.; grant 01GM2209F to L.S. and S.H.), the National Institute of Neurological Disorders and Stroke (NINDS)/National Institutes of Health (NIH) under Award Number R01NS072248 (grant to R.S.), the European Health and Digital Executive Agency (HADEA) through funding for the European Rare Disease Research Alliance (ERDERA; grant agreement 101156595 to R.S.) and the Clinician Scientist Programme PRECISE.net funded by the Else Kröner-Fresenius-Stiftung (grant to R.S.). R.S. and L.S. are members of the European Reference Network for Rare Neurological Diseases—Project ID 739510. NGS sequencing methods were performed with the support of the DFG-funded NGS Competence Center Tübingen (INST 37/1049-1). For the publication fee we acknowledge financial support by Heidelberg University.

Acknowledgements. We would like to thank Jessica Cielenga for her technical support.

## References

1. Bentley M, Banker G. 2016 The cellular mechanisms that maintain neuronal polarity. *Nat. Rev. Neurosci.* **17**, 611–622. (doi:10.1038/nrn.2016.100)
2. Sutton MA, Schuman EM. 2006 Dendritic protein synthesis, synaptic plasticity, and memory. *Cell* **127**, 49–58. (doi:10.1016/j.cell.2006.09.014)
3. Wang DO, Martin KC, Zukin RS. 2010 Spatially restricting gene expression by local translation at synapses. *Trends Neurosci.* **33**, 173–182. (doi:10.1016/j.tins.2010.01.005)
4. Perry RB, Fainzilber M. 2014 Local translation in neuronal processes—*in vivo* tests of a 'heretical hypothesis'. *Dev. Neurobiol.* **74**, 210–217. (doi:10.1002/dneu.22115)
5. Tom Dieck S, Hanus C, Schuman EM. 2014 SnapShot: local protein translation in dendrites. *Neuron* **81**, 958–958. (doi:10.1016/j.neuron.2014.02.009)
6. Li H, Li SH, Yu ZX, Shelbourne P, Li XJ. 2001 Huntingtin aggregate-associated axonal degeneration is an early pathological event in Huntington's disease mice. *J. Neurosci.* **21**, 8473–8481. (doi:10.1523/JNEUROSCI.21-21-08473.2001)
7. Ferri A, Sanes JR, Coleman MP, Cunningham JM, Kato AC. 2003 Inhibiting axon degeneration and synapse loss attenuates apoptosis and disease progression in a mouse model of motoneuron disease. *Curr. Biol.* **13**, 669–673. (doi:10.1016/s0960-9822(03)00206-9)

8. Fischer LR, Culver DG, Tennant P, Davis AA, Wang M, Castellano-Sanchez A, Khan J, Polak MA, Glass JD. 2004 Amyotrophic lateral sclerosis is a distal axonopathy: evidence in mice and man. *Exp. Neurol.* **185**, 232–240. (doi:10.1016/j.expneurol.2003.10.004)
9. Libby RT, Li Y, Savinova OV, Barter J, Smith RS, Nickells RW, John SW. 2005 Susceptibility to neurodegeneration in a glaucoma is modified by Bax gene dosage. *PLoS Genet.* **1**, 17–26. (doi:10.1371/journal.pgen.0010004)
10. Stokin GB *et al*. 2005 Axonopathy and transport deficits early in the pathogenesis of Alzheimer's disease. *Science* **307**, 1282–1288. (doi:10.1126/science.1105681)
11. Hörner M *et al*. 2022 CNS-associated T-lymphocytes in a mouse model of hereditary spastic paraplegia type 11 (SPG11) are therapeutic targets for established immunomodulators. *Exp. Neurol.* **355**, 114119. (doi:10.1016/j.expneurol.2022.114119)
12. Zivraj KH, Tung YC, Piper M, Gumy L, Fawcett JW, Yeo GS, Holt CE. 2010 Subcellular profiling reveals distinct and developmentally regulated repertoire of growth cone mRNAs. *J. Neurosci.* **30**, 15464–15478. (doi:10.1523/JNEUROSCI.1800-10.2010)
13. Gumy LF *et al*. 2011 Transcriptome analysis of embryonic and adult sensory axons reveals changes in mRNA repertoire localization. *RNA* **17**, 85–98. (doi:10.1261/rna.2386111)
14. Nijssen J, Aguila J, Hoogstraaten R, Kee N, Hedlund E. 2018 Axon-Seq decodes the motor axon transcriptome and its modulation in response to ALS. *Stem Cell Rep.* **11**, 1565–1578. (doi:10.1016/j.stemcr.2018.11.005)
15. Minis A, Dahary D, Manor O, Leshkowitz D, Pilpel Y, Yaron A. 2014 Subcellular transcriptomics-dissection of the mRNA composition in the axonal compartment of sensory neurons. *Dev. Neurobiol.* **74**, 365–381. (doi:10.1002/dneu.22140)
16. Briese M, Saal L, Appenzeller S, Moradi M, Baluapuri A, Sendtner M. 2016 Whole transcriptome profiling reveals the RNA content of motor axons. *Nucleic Acids Res.* **44**, e33. (doi:10.1093/nar/gkv1027)
17. Kopp P, Lammers R, Aepfelbacher M, Woehlke G, Rudel T, Machuy N, Steffen W, Linder S. 2006 The kinesin KIF1C and microtubule plus ends regulate podosome dynamics in macrophages. *Mol. Biol. Cell* **17**, 2811–2823. (doi:10.1091/mbc.e05-11-1010)
18. del Rio R, McAllister RD, Meeker ND, Wall EH, Bond JP, Kyttaris VC, Tsokos GC, Tung KS, Teuscher C. 2012 Identification of Orch3, a locus controlling dominant resistance to autoimmune orchitis, as kinesin family member 1C. *PLoS Genet.* **8**, e1003140. (doi:10.1371/journal.pgen.1003140)
19. Simpson JC *et al*. 2012 Genome-wide RNAi screening identifies human proteins with a regulatory function in the early secretory pathway. *Nat. Cell Biol.* **14**, 764–774. (doi:10.1038/ncb2510)
20. Theisen U, Straube E, Straube A. 2012 Directional persistence of migrating cells requires Kif1C-mediated stabilization of trailing adhesions. *Dev. Cell* **23**, 1153–1166. (doi:10.1016/j.devcel.2012.11.005)
21. Bhuwania R, Castro-Castro A, Linder S. 2014 Microtubule acetylation regulates dynamics of KIF1C-powered vesicles and contact of microtubule plus ends with podosomes. *Eur. J. Cell Biol.* **93**, 424–437. (doi:10.1016/j.ejcb.2014.07.006)
22. Efimova N, Grimaldi A, Bachmann A, Frye K, Zhu X, Feoktistov A, Straube A, Kaverina I. 2014 Podosome-regulating kinesin KIF1C translocates to the cell periphery in a CLASP-dependent manner. *J. Cell. Sci.* **127**, 5179–5188. (doi:10.1242/jcs.149633)
23. Lee PL, Ohlson MB, Pfeffer SR. 2015 Rab6 regulation of the kinesin family KIF1C motor domain contributes to golgi tethering. *eLife* **4**, e06029. (doi:10.7554/eLife.06029)
24. Pichon X *et al*. 2021 The kinesin KIF1C transports APC-dependent mRNAs to cell protrusions. *RNA* **27**, 1528–1544. (doi:10.1261/rna.078576.120)
25. Nagel M, Noss M, Xu J, Horn N, Ueffing M, Boldt K, Schuele R. 2022 The kinesin motor KIF1C is a putative transporter of the exon junction complex in neuronal cells. *RNA* **29**, 55–68. (doi:10.1261/rna.079426.122)
26. Norris ML, Mendell JT. 2023 Localization of Kif1c mRNA to cell protrusions dictates binding partner specificity of the encoded protein. *Genes Dev.* **37**, 191–203. (doi:10.1101/gad.350320.122)
27. De Pace R *et al*. 2024 Messenger RNA transport on lysosomal vesicles maintains axonal mitochondrial homeostasis and prevents axonal degeneration. *Nat. Neurosci.* **27**, 1087–1102. (doi:10.1038/s41593-024-01619-1)
28. Maciel R, Bis DM, Rebelo AP, Saghira C, Züchner S, Saporta MA. 2018 The human motor neuron axonal transcriptome is enriched for transcripts related to mitochondrial function and microtubule-based axonal transport. *Exp. Neurol.* **307**, 155–163. (doi:10.1016/j.expneurol.2018.06.008)
29. Rubin CI, Atweh GF. 2004 The role of stathmin in the regulation of the cell cycle. *J. Cell. Biochem.* **93**, 242–250. (doi:10.1002/jcb.20187)
30. Thornburg-Suresh EJC, Richardson JE, Summers DW. 2023 The stathmin-2 membrane-targeting domain is required for axon protection and regulated degradation by DLK signaling. *J. Biol. Chem.* **299**, 104861. (doi:10.1016/j.jbc.2023.104861)
31. López-Erauskin J *et al*. 2024 Stathmin-2 loss leads to neurofilament-dependent axonal collapse driving motor and sensory denervation. *Nat. Neurosci.* **27**, 34–47. (doi:10.1038/s41593-023-01496-0)
32. Denny JB. 2006 Molecular mechanisms, biological actions, and neuropharmacology of the growth-associated protein GAP-43. *Curr. Neuropharmacol.* **4**, 293–304. (doi:10.2174/157015906778520782)
33. Chung D, Shum A, Caraveo G. 2020 GAP-43 and BASP1 in axon regeneration: implications for the treatment of neurodegenerative diseases. *Front. Cell Dev. Biol.* **8**, 567537. (doi:10.3389/fcell.2020.567537)
34. Cox LJ, Hengst U, Gurskaya NG, Lukyanov KA, Jaffrey SR. 2008 Intra-axonal translation and retrograde trafficking of CREB promotes neuronal survival. *Nat. Cell Biol.* **10**, 149–159.
35. Wizenmann A *et al*. 2009 Extracellular Engrailed participates in the topographic guidance of retinal axons in vivo. *Neuron* **64**, 355–366. (doi:10.1016/j.neuron.2009.09.018)
36. Ben-Yaakov K *et al*. 2012 Axonal transcription factors signal retrogradely in lesioned peripheral nerve. *EMBO J.* **31**, 1350–1363. (doi:10.1038/emboj.2011.494)
37. Ji SJ, Jaffrey SR. 2012 Intra-axonal translation of SMAD1/5/8 mediates retrograde regulation of trigeminal ganglia subtype specification. *Neuron* **74**, 95–107. (doi:10.1016/j.neuron.2012.02.022)
38. Guillaud L, El-Agamy SE, Otsuki M, Terenzio M. 2020 Anterograde axonal transport in neuronal homeostasis and disease. *Front. Mol. Neurosci.* **13**, 556175. (doi:10.3389/fnmol.2020.556175)
39. Leboeuf M, Vargas-Abonce SE, Pezé-Hedsieck E, Dupont E, Jimenez-Alonso L, Moya KL, Prochiantz A. 2023 ENGRAILED-1 transcription factor has a paracrine neurotrophic activity on adult spinal α-motoneurons. *EMBO Rep.* **24**, e56525. (doi:10.15252/embr.202256525)
40. Shen WK, Chen SY, Gan ZQ, Zhang YZ, Yue T, Chen MM, Xue Y, Hu H, Guo AY. 2023 AnimalTFDB 4.0: a comprehensive animal transcription factor database updated with variation and expression annotations. *Nucleic Acids Res.* **51**, D39–D45. (doi:10.1093/nar/gkac907)
41. Seifart KH, Wang L, Waldschmidt R, Jahn D, Wingender E. 1989 Purification of human transcription factor IIIA and its interaction with a chemically synthesized gene encoding human 5 S rRNA. *J. Biol. Chem.* **264**, 1702–1709.
42. Anuraga G, Tang WC, Phan NN, Ta HDK, Liu YH, Wu YF, Lee KH, Wang CY. 2021 Comprehensive analysis of prognostic and genetic signatures for general transcription factor III (GTF3) in clinical colorectal cancer patients using bioinformatics approaches. *Curr. Issues Mol. Biol.* **43**, 2–20. (doi:10.3390/cimb43010002)

43. Hasmatali JCD, De Guzman J, Zhai R, Yang L, McLean NA, Hutchinson C, Johnston JM, Misra V, Verge VMK. 2019 Axotomy induces phasic alterations in Luman/CREB3 expression and nuclear localization in injured and contralateral uninjured sensory neurons: correlation with intrinsic axon growth capacity. *J. Neuropathol. Exp. Neurol.* **78**, 348–364. (doi:10.1093/jnen/nlz008)
44. Sampieri L, Di Giusto P, Alvarez C. 2019 CREB3 transcription factors: ER-Golgi stress transducers as hubs for cellular homeostasis. *Front. Cell Dev. Biol.* **7**, 123. (doi:10.3389/fcell.2019.00123)
45. Contreras A, Hines DJ, Hines RM. 2019 Molecular specialization of GABAergic synapses on the soma and axon in cortical and hippocampal circuit function and dysfunction. *Front. Mol. Neurosci.* **12**, 154. (doi:10.3389/fnmol.2019.00154)
46. Kozar-Gillan N *et al*. 2023 LGI3/2-ADAM23 interactions cluster Kv1 channels in myelinated axons to regulate refractory period. *J. Cell Biol.* **222**, e202211031. (doi:10.1083/jcb.202211031)
47. Srinivasan R, Jang SW, Ward RM, Sachdev S, Ezashi T, Svaren J. 2007 Differential regulation of NAB corepressor genes in Schwann cells. *BMC Mol. Biol.* **8**, 117. (doi:10.1186/1471-2199-8-117)
48. Chia PH, Patel MR, Shen K. 2012 NAB-1 instructs synapse assembly by linking adhesion molecules and F-actin to active zone proteins. *Nat. Neurosci.* **15**, 234–242. (doi:10.1038/nn.2991)
49. El Soury M *et al*. 2018 Soluble neuregulin1 down-regulates myelination genes in Schwann cells. *Front. Mol. Neurosci.* **11**, 157. (doi:10.3389/fnmol.2018.00157)
50. Jia Y, Jucius TJ, Cook SA, Ackerman SL. 2015 Loss of Clcc1 results in ER stress, misfolded protein accumulation, and neurodegeneration. *J. Neurosci.* **35**, 3001–3009. (doi:10.1523/JNEUROSCI.3678-14.2015)
51. Cheng F *et al*. 2020 Unraveling molecular mechanisms of THAP1 missense mutations in DYT6 dystonia. *J. Mol. Neurosci.* **70**, 999–1008. (doi:10.1007/s12031-020-01490-2)
52. Yim YS, Kwon Y, Nam J, Yoon HI, Lee K, Kim DG, Kim E, Kim CH, Ko J. 2013 Slitrks control excitatory and inhibitory synapse formation with LAR receptor protein tyrosine phosphatases. *Proc. Natl Acad. Sci. USA* **110**, 4057–4062. (doi:10.1073/pnas.1209881110)
53. Preitner N, Quan J, Nowakowski DW, Hancock ML, Shi J, Tcherkezian J, Young-Pearse TL, Flanagan JG. 2014 APC is an RNA-binding protein, and its interactome provides a link to neural development and microtubule assembly. *Cell* **158**, 368–382. (doi:10.1016/j.cell.2014.05.042)
54. Rotem N *et al*. 2017 ALS along the axons: expression of coding and noncoding RNA differs in axons of ALS models. *Sci. Rep.* **7**, 44500. (doi:10.1038/srep44500)
55. Li L, Yu J, Ji SJ. 2021 Axonal mRNA localization and translation: local events with broad roles. *Cell. Mol. Life Sci.* **78**, 7379–7395. (doi:10.1007/s00018-021-03995-4)
56. Koppers M *et al*. 2019 Receptor-specific interactome as a hub for rapid cue-induced selective translation in axons. *eLife* **8**, e48718. (doi:10.7554/eLife.48718)
57. Sasaki Y, Welshhans K, Wen Z, Yao J, Xu M, Goshima Y, Zheng JQ, Bassell GJ. 2010 Phosphorylation of zipcode binding protein 1 is required for brain-derived neurotrophic factor signaling of local beta-actin synthesis and growth cone turning. *J. Neurosci.* **30**, 9349–9358. (doi:10.1523/JNEUROSCI.0499-10.2010)
58. Sonenberg N, Hinnebusch AG. 2009 Regulation of translation initiation in eukaryotes: mechanisms and biological targets. *Cell* **136**, 731–745. (doi:10.1016/j.cell.2009.01.042)
59. Hornberg H, Holt C. 2013 RNA-binding proteins and translational regulation in axons and growth cones. *Front. Neurosci.* **7**, 81. (doi:10.3389/fnins.2013.00081)
60. Moccia R *et al*. 2003 An unbiased cDNA library prepared from isolated *Aplysia* sensory neuron processes is enriched for cytoskeletal and translational mRNAs. *J. Neurosci.* **23**, 9409–9417. (doi:10.1523/JNEUROSCI.23-28-09409.2003)
61. Poon MM, Choi SH, Jamieson CA, Geschwind DH, Martin KC. 2006 Identification of process-localized mRNAs from cultured rodent hippocampal neurons. *J. Neurosci.* **26**, 13390–13399. (doi:10.1523/JNEUROSCI.3432-06.2006)
62. Zhong J, Zhang T, Bloch LM. 2006 Dendritic mRNAs encode diversified functionalities in hippocampal pyramidal neurons. *BMC Neurosci.* **7**, 17. (doi:10.1186/1471-2202-7-17)
63. Taylor AM, Berchtold NC, Perreau VM, Tu CH, Li Jeon N, Cotman CW. 2009 Axonal mRNA in uninjured and regenerating cortical mammalian axons. *J. Neurosci.* **29**, 4697–4707. (doi:10.1523/JNEUROSCI.6130-08.2009)
64. Andreassi C, Zimmermann C, Mitter R, Fusco S, De Vita S, Saiardi A, Riccio A. 2010 An NGF-responsive element targets myo-inositol monophosphatase-1 mRNA to sympathetic neuron axons. *Nat. Neurosci.* **13**, 291–301. (doi:10.1038/nn.2486)
65. Jung H, Gkogkas CG, Sonenberg N, Holt CE. 2014 Remote control of gene function by local translation. *Cell* **157**, 26–40. (doi:10.1016/j.cell.2014.03.005)
66. Shigeoka T *et al*. 2019 On-site ribosome remodeling by locally synthesized ribosomal proteins in axons. *Cell Rep.* **29**, 3605–3619. (doi:10.1016/j.celrep.2019.11.025)
67. Wei M *et al*. 2021 Axon-enriched lincRNA ALAE is required for axon elongation via regulation of local mRNA translation. *Cell Rep.* **35**, 109053. (doi:10.1016/j.celrep.2021.109053)
68. Donnelly CJ *et al*. 2013 Axonally synthesized beta-actin and GAP-43 proteins support distinct modes of axonal growth. *J. Neurosci.* **33**, 3311–3322. (doi:10.1523/JNEUROSCI.1722-12.2013)
69. Sgadò P, Albéri L, Gherbassi D, Galasso SL, Ramakers GMJ, Alavian KN, Smidt MP, Dyck RH, Simon HH. 2006 Slow progressive degeneration of nigral dopaminergic neurons in postnatal engrailed mutant mice. *Proc. Natl Acad. Sci. USA* **103**, 15242–15247. (doi:10.1073/pnas.0602116103)
70. Sugiyama S, Di Nardo AA, Aizawa S, Matsuo I, Volovitch M, Prochiantz A, Hensch TK. 2008 Experience-dependent transfer of Otx2 homeoprotein into the visual cortex activates postnatal plasticity. *Cell* **134**, 508–520. (doi:10.1016/j.cell.2008.05.054)
71. Torero Ibad R, Rheey J, Mrejen S, Forster V, Picaud S, Prochiantz A, Moya KL. 2011 Otx2 promotes the survival of damaged adult retinal ganglion cells and protects against excitotoxic loss of visual acuity in vivo. *J. Neurosci.* **31**, 5495–5503. (doi:10.1523/JNEUROSCI.0187-11.2011)
72. Kadkhodaei B *et al*. 2013 Transcription factor Nurr1 maintains fiber integrity and nuclear-encoded mitochondrial gene expression in dopamine neurons. *Proc. Natl Acad. Sci. USA* **110**, 2360–2365. (doi:10.1073/pnas.1221077110)
73. Huang JK, Jarjour AA, Ffrench-Constant C, Franklin RJ. 2011 Retinoid X receptors as a potential avenue for regenerative medicine in multiple sclerosis. *Expert Rev. Neurother.* **11**, 467–468. (doi:10.1586/ern.11.34)
74. Hengst U, Jaffrey SR. 2007 Function and translational regulation of mRNA in developing axons. *Semin. Cell Dev. Biol.* **18**, 209–215. (doi:10.1016/j.semcdb.2007.01.003)
75. Hengst U, Deglincerti A, Kim HJ, Jeon NL, Jaffrey SR. 2009 Axonal elongation triggered by stimulus-induced local translation of a polarity complex protein. *Nat. Cell Biol.* **11**, 1024–1030. (doi:10.1038/ncb1916)
76. Gracias NG, Shirkey-Son NJ, Hengst U. 2014 Local translation of TC10 is required for membrane expansion during axon outgrowth. *Nat. Commun.* **5**, 3506. (doi:10.1038/ncomms4506)
77. Lyabin DN, Eliseeva IA, Ovchinnikov LP. 2014 YB-1 protein: functions and regulation. *Wiley Interdiscip. Rev. RNA* **5**, 95–110. (doi:10.1002/wrna.1200)
78. Kar AN, Vargas JNS, Chen CY, Kowalak JA, Gioio AE, Kaplan BB. 2017 Molecular determinants of cytochrome C oxidase IV mRNA axonal trafficking. *Mol. Cell. Neurosci.* **80**, 32–43. (doi:10.1016/j.mcn.2017.01.008)
79. Trinh MA, Kaphzan H, Wek RC, Pierre P, Cavener DR, Klann E. 2012 Brain-specific disruption of the eIF2alpha kinase PERK decreases ATF4 expression and impairs behavioral flexibility. *Cell Rep.* **1**, 676–688. (doi:10.1016/j.celrep.2012.04.010)

80. Baleriola J, Walker CA, Jean YY, Crary JF, Troy CM, Nagy PL, Hengst U. 2014 Axonally synthesized ATF4 transmits a neurodegenerative signal across brain regions. *Cell* **158**, 1159–1172. (doi:10.1016/j.cell.2014.07.001)
81. Vasudevan D, Neuman SD, Yang A, Lough L, Brown B, Bashirullah A, Cardozo T, Ryoo HD. 2020 Translational induction of ATF4 during integrated stress response requires noncanonical initiation factors eIF2D and DENR. *Nat. Commun.* **11**, 4677. (doi:10.1038/s41467-020-18453-1)
82. Stevanin G, Ruberg M, Brice A. 2008 Recent advances in the genetics of spastic paraplegias. *Curr. Neurol. Neurosci. Rep.* **8**, 198–210. (doi:10.1007/s11910-008-0032-z)
83. Caballero Oteyza A *et al*. 2014 Motor protein mutations cause a new form of hereditary spastic paraplegia. *Neurology* **82**, 2007–2016. (doi:10.1212/WNL.0000000000000479)
84. Dor T *et al*. 2014 KIF1C mutations in two families with hereditary spastic paraparesis and cerebellar dysfunction. *J. Med. Genet.* **51**, 137–142. (doi:10.1136/jmedgenet-2013-102012)
85. Novarino G *et al*. 2014 Exome sequencing links corticospinal motor neuron disease to common neurodegenerative disorders. *Science* **343**, 506–511. (doi:10.1126/science.1247363)
86. Klebe S, Stevanin G, Depienne C. 2015 Clinical and genetic heterogeneity in hereditary spastic paraplegias: from SPG1 to SPG72 and still counting. *Rev. Neurol.* **171**, 505–530. (doi:10.1016/j.neurol.2015.02.017)
87. Blackstone C. 2018 Hereditary spastic paraplegia. *Handb. Clin. Neurol.* **148**, 633–652. (doi:10.1016/B978-0-444-64076-5.00041-7)
88. Lipka J, Kapitein LC, Jaworski J, Hoogenraad CC. 2016 Microtubule-binding protein doublecortin-like kinase 1 (DCLK1) guides kinesin-3-mediated cargo transport to dendrites. *EMBO J.* **35**, 302–318. (doi:10.15252/embj.201592929)
89. Perlson E, Maday S, Fu MM, Moughamian AJ, Holzbaur EL. 2010 Retrograde axonal transport: pathways to cell death? *Trends Neurosci.* **33**, 335–344. (doi:10.1016/j.tins.2010.03.006)
90. Millecamps S, Julien JP. 2013 Axonal transport deficits and neurodegenerative diseases. *Nat. Rev. Neurosci.* **14**, 161–176. (doi:10.1038/nrn3380)
91. Puls I *et al*. 2003 Mutant dynactin in motor neuron disease. *Nat. Genet.* **33**, 455–456. (doi:10.1038/ng1123)
92. Münch C *et al*. 2004 Point mutations of the p150 subunit of dynactin (DCTN1) gene in ALS. *Neurology* **63**, 724–726. (doi:10.1212/01.wnl.0000134608.83927.b1)
93. Weedon MN *et al*. 2011 Exome sequencing identifies a DYNC1H1 mutation in a large pedigree with dominant axonal Charcot–Marie–Tooth disease. *Am. J. Hum. Genet.* **89**, 308–312. (doi:10.1016/j.ajhg.2011.07.002)
94. Cady J *et al*. 2015 Amyotrophic lateral sclerosis onset is influenced by the burden of rare variants in known amyotrophic lateral sclerosis genes. *Ann. Neurol.* **77**, 100–113. (doi:10.1002/ana.24306)
95. Konno T, Ross OA, Teive HAG, Sławek J, Dickson DW, Wszolek ZK. 2017 DCTN1-related neurodegeneration: perry syndrome and beyond. *Parkinsonism Relat. Disord.* **41**, 14–24. (doi:10.1016/j.parkreldis.2017.06.004)
96. Singer RH. 1993 RNA zipcodes for cytoplasmic addresses. *Curr. Biol.* **3**, 719–721. (doi:10.1016/0960-9822(93)90079-4)
97. Latham VM, Yu EH, Tullio AN, Adelstein RS, Singer RH. 2001 A Rho-dependent signaling pathway operating through myosin localizes beta-actin mRNA in fibroblasts. *Curr. Biol.* **11**, 1010–1016. (doi:10.1016/s0960-9822(01)00291-3)
98. Fusco D, Accornero N, Lavoie B, Shenoy SM, Blanchard JM, Singer RH, Bertrand E. 2003 Single mRNA molecules demonstrate probabilistic movement in living mammalian cells. *Curr. Biol.* **13**, 161–167. (doi:10.1016/s0960-9822(02)01436-7)
99. Oleynikov Y, Singer RH. 2003 Real-time visualization of ZBP1 association with beta-actin mRNA during transcription and localization. *Curr. Biol.* **13**, 199–207. (doi:10.1016/s0960-9822(03)00044-7)
100. Condeelis J, Singer RH. 2005 How and why does beta-actin mRNA target? *Biol. Cell* **97**, 97–110. (doi:10.1042/BC20040063)
101. Ma B, Savas JN, Yu MS, Culver BP, Chao MV, Tanese N. 2011 Huntingtin mediates dendritic transport of beta-actin mRNA in rat neurons. *Sci. Rep.* **1**, 140. (doi:10.1038/srep00140)
102. Nalavadi VC, Griffin LE, Picard-Fraser P, Swanson AM, Takumi T, Bassell GJ. 2012 Regulation of zipcode binding protein 1 transport dynamics in axons by myosin Va. *J. Neurosci.* **32**, 15133–15141. (doi:10.1523/JNEUROSCI.2006-12.2012)
103. Liao G, Mingle L, Van De Water L, Liu G. 2015 Control of cell migration through mRNA localization and local translation. *Wiley Interdiscip. Rev. RNA* **6**, 1–15. (doi:10.1002/wrna.1265)
104. Song T, Zheng Y, Wang Y, Katz Z, Liu X, Chen S, Singer RH, Gu W. 2015 Specific interaction of KIF11 with ZBP1 regulates the transport of beta-actin mRNA and cell motility. *J. Cell. Sci.* **128**, 1001–1010. (doi:10.1242/jcs.161679)
105. Wang T, Hamilla S, Cam M, Aranda-Espinoza H, Mili S. 2017 Extracellular matrix stiffness and cell contractility control RNA localization to promote cell migration. *Nat. Commun.* **8**, 896. (doi:10.1038/s41467-017-00884-y)
106. Nagel M, Mussig S, Hoflinger P, Schols L, Hauser S, Schüle R. 2020 Generation of the CRISPR/Cas9-mediated KIF1C knock-out human iPSC line HIHRSi003-A-1. *Stem Cell Res.* **49**, 102059. (doi:10.1016/j.scr.2020.102059)
107. Hauser S *et al*. 2020 Comparative transcriptional profiling of motor neuron disorder-associated genes in various human cell culture models. *Front. Cell Dev. Biol.* **8**, 544043. (doi:10.3389/fcell.2020.544043)
108. Schuster S, Heuten E, Velic A, Admard J, Synofzik M, Ossowski S, Macek B, Hauser S, Schols L. 2020 CHIP mutations affect the heat shock response differently in human fibroblasts and iPSC-derived neurons. *Dis. Model. Mech.* **13**, dmm045096. (doi:10.1242/dmm.045096)
109. Dobin A, Davis CA, Schlesinger F, Drenkow J, Zaleski C, Jha S, Batut P, Chaisson M, Gingeras TR. 2013 STAR: ultrafast universal RNA-seq aligner. *Bioinformatics* **29**, 15–21. (doi:10.1093/bioinformatics/bts635)
110. Liao Y, Smyth GK, Shi W. 2014 featureCounts: an efficient general purpose program for assigning sequence reads to genomic features. *Bioinformatics* **30**, 923–930. (doi:10.1093/bioinformatics/btt656)
111. Xu J, Hörner M, Nagel M, Perhat P, Korneck M, Noß M. 2025 Supplementary Material from: Unraveling Axonal Transcriptional Landscapes: Insights from iPSC-Derived Cortical Neurons and Implications for Motor Neuron Degeneration. Figshare. (doi:10.6084/m9.figshare.c.7819460)